

# Geodetic techniques for time and frequency comparisons using GPS phase and code measurements

Jim Ray<sup>1</sup> and Ken Senior<sup>2</sup>

<sup>1</sup> US National Geodetic Survey, NOAA N/NGS6, Silver Spring, MD, USA, and  
Bureau International des Poids et Mesures, Sèvres, France

<sup>2</sup> US Naval Research Laboratory, Code 8154, Washington, DC, USA

Received 16 December 2004

Published 26 April 2005

Online at [stacks.iop.org/Met/42/215](http://stacks.iop.org/Met/42/215)

## Abstract

We review the development and status of GPS geodetic methods for high-precision global time and frequency comparisons. A comprehensive view is taken, including hardware effects in the transmitting satellites and tracking receiver stations, data analysis and interpretation, and comparisons with independent results. Other GPS techniques rely on single-frequency data and/or assume cancellation of most systematic errors using differences between simultaneous observations. By applying the full observation modelling of modern geodesy to dual-frequency observations of GPS carrier phase and pseudorange, the precision of timing comparisons can be improved from the level of several nanoseconds to near 100 ps. For an averaging interval of one day, we infer a limiting Allan deviation of about  $1.4 \times 10^{-15}$  for the GPS geodetic technique. The accuracy of time comparisons is set by the ability to calibrate the absolute instrumental delays through the GPS receiver and antenna chain, currently about 3 ns. Geodetic clock measurements are available for most of the major timing laboratories, as well as for many other tracking stations and the satellites, via the routine products of the International GPS Service.

(Some figures in this article are in colour only in the electronic version)

## 1. Introduction

GPS methods have been the basis for most high-accuracy time and frequency transfers for more than two decades. The usual approach for maintaining Coordinated Universal Time (UTC) has relied primarily on single-frequency pseudorange (C/A-code) data and simple common-view (CV) data analyses that assume cancellation of most systematic errors [1]. With improved data yields thanks to widespread replacement of the earlier single-channel receivers by multi-channel units, intercontinental CV comparisons have achieved uncertainties of a few nanoseconds averaged over five-day intervals [2]. Other incremental refinements to the CV method continue to be applied. In contrast, the parallel development of high-accuracy geodetic methods using dual-frequency GPS carrier-phase observables has demonstrated positioning repeatabilities at the centimetre level for one-day integrations [3]. Assuming such positioning results can

also be realized as equivalent light travel times ( $\sim 33$  ps), the potential for GPS carrier phase-based geodetic techniques to permit sub-nanosecond global time comparisons is evident, as widely recognized by the 1990s [4]. In fact, the method has been shown to have a precision approaching  $\sim 100$  ps at each epoch in favourable cases for one-day analysis arcs [5]. The absolute time transfer capability remains limited to  $> 1$  ns, however, due to instrumental calibration uncertainties [6]. In addition to higher precision (equivalent to frequency stability), the geodetic approach easily lends itself to global one-way time and frequency dissemination. This is consistent with the basic GPS operational design (albeit with replacement of the GPS broadcast message with more accurate information), unlike the point-to-point nature of CV, which furthermore degrades as baseline distances increase.

The essential ingredients of the geodetic method are the availability of dual-frequency GPS observations for both pseudorange (usually ‘codeless’ P-code) and carrier phase,



GPS broadcasts are currently within two L-bands, having nominal central frequencies of  $L_1 = 154 \times 10.23 = 1575.42$  MHz and  $L_2 = 120 \times 10.23 = 1227.60$  MHz. The  $L_1$  band contains a 1.023 MHz coarse acquisition (C/A) code modulation as well as an encrypted P1(Y) code (10.23 MHz) and a 50 bps message code. On  $L_2$  only a precise 10.23 MHz P2(Y) code is currently modulated, though a second civilian code is to be added in the near future. While nominally in phase, the various GPS modulations inevitably have significant non-zero biases with respect to one another. The most important of these is the pseudorange bias between the P1 and P2 modulations. The peak-to-peak dispersion in P1–P2 biases is more than 10 ns. Since the broadcast clocks are determined for the ionosphere-free P1/P2 linear combination (see more below), single-frequency users must compensate for the P1–P2 biases by using the  $T_{GD}$  group delay biases given in the navigation message (see ICD-GPS-200). In generating its ionospheric map products, the IGS also reports its own observed P1–P2 biases, known as differential code biases (DCBs). For reference, the nominal relationship between broadcast  $T_{GD}$  values and IGS DCBs is given by

$$DCB = \left[ 1 - \left( \frac{77}{60} \right)^2 \right] * T_{GD} \quad (+ \text{scale offset})$$

for each individual satellite, except that the two scales differ by a time-varying offset because the mean value for DCBs is set by IGS convention to zero whereas the broadcast  $T_{GD}$  values are referenced to an empirical absolute instrumental bias. The scale difference, in  $T_{GD}$  units, has gradually been decreasing, from about  $-4.3$  ns at the beginning of 2000 to  $-7.1$  ns in mid-2004 as the constellation evolves and new satellites with different biases are launched. The broadcast  $T_{GD}$  values are reviewed and updated quarterly, while the IGS monitors and reports its DCBs continuously at daily intervals.

The  $T_{GD}$  correction procedure assumes the P1–P2 bias is appropriate for single-frequency users of the C/A-code, the same as for P1. In fact, this is not strictly true because of P1–C/A biases. They have a peak-to-peak range of about 5 ns. While currently ignored in ICD-GPS-200, the IGS has accounted for such biases since 1999. It is necessary because some geodetic receivers track C/A instead of P1 and some report  $[C/A + (P2-P1)]$  instead of true P2, which have different biases [9]. To avoid mixing data with different satellite biases, which would degrade the IGS satellite clock products (and precise point positioning (PPP) using them), procedures for handling and analysing diverse GPS data sets were implemented by the IGS to maintain consistency. As new modulations are added to the GPS signals in the future, it is expected that calibration values for the additional inter-signal biases will be included in the broadcast navigation message and monitored by the IGS.

Another complication of the satellite transmit signals is the phase pattern of the beam. While it is generally assumed to be perfectly hemispherical, there is strong evidence otherwise [10]. Neglect of the non-ideal phase patterns, for satellites or tracking antennas (see more below), causes mostly errors in the GPS frame scale (i.e. radial direction) at the level of roughly 10–15 parts per billion (ppb). While this is important for many geodetic applications, this effect is probably not significant for most time comparisons, at least not until instrumental calibrations attain sub-nanosecond accuracy.

A final point to note concerning the GPS satellite clocks is that the intentional degradation of the GPS clock signals by selective availability (SA) was discontinued at 04:00 UTC on 02 May 2000. Prior to that time, the RMS clock variations over a day were at the level of roughly 80 ns. Since then, the clock stability is that intrinsic to each satellite's timekeeping system, which is more than an order of magnitude better. In addition to allowing civilian access to greatly improved GPS positioning and timing determinations, all users, especially those taking advantage of the much more accurate IGS products, can now interpolate tabulated GPS clock values with far smaller errors than before.

## 2.2. GPS tracking antenna installations

A geodetic installation is normally built about an ultra-stable monument that provides the physical basis for long-term, high-accuracy measurements. Deeply anchored concrete piers, cross-braced metal rod structures and steel masts are among the monument designs commonly used, although buildings are also used, especially for timing applications. Information about various monument types is available at [igs.cb.jpl.nasa.gov/network/monumentation.html](http://igs.cb.jpl.nasa.gov/network/monumentation.html). Permanently and securely embedded into the monument is a geodetic marker with an inscribed point to which the station coordinates are referred. The best practice is to also establish a high-accuracy local geodetic control network to monitor relative motions of the primary GPS station. In order to distinguish very local monument displacements from larger-scale effects, the control network should include permanent markers covering a range of distances from  $\sim 10$ –100 m out to around 10 km. The local network must be resurveyed periodically to be useful and may be partly formed by other continuously operating GPS stations. The GPS antenna itself should be securely anchored directly over the geodetic marker in such a way that its position is fixed and the eccentricity from the marker reference point to the antenna reference point (ARP) can be measured with an accuracy  $< 1$  mm. A conventional ARP has been designated by the IGS for each antenna model. It must be a physically accessible point, as opposed to the L1 and L2 electrical phase centres, for local survey measurements to be made. For most choke ring antennas, the ARP is a point at the base of the preamplifier on the bottom side of the unit. The physical dimensions relating the ARP and the signal phase centres, as well as measured wavefront phase patterns, are maintained in files available from the IGS. The information on marker eccentricity and antenna dimensions is required to analyse the observational data and reduce the results to the reference station coordinates.

In cases where the highest quality geodetic performance is not required, such as many timing installations, a geodetic monument and marker might not be used. In this situation, the station coordinates are referenced directly to the ARP (or sometimes to the phase centre). While this is expedient, this will generally cause a station's coordinates to change whenever the antenna model is changed. It is preferable to follow standard geodetic guidelines whenever practical. In any case, the stability of the antenna mount is important because its variations (e.g. due to solar heating of a steel mast) will induce corresponding effects in the estimated clocks.

High-quality, dual-frequency antennas are required for geodetic applications, including high-accuracy time transfer. The most common design features a set of concentric choke rings, available from several vendors with slightly different internal dimensions. The design has been tailored for dual-frequency reception while strongly attenuating signals near the horizon and below, where multi-path reflections are usually worst [11]. For time transfer applications, in particular, it is critical that the antenna be situated in such a way as to minimize multi-path signals, especially code multi-path. Generally, this means maintaining a clear horizon in all directions and avoiding placement of reflecting objects near the antenna. The L2 signal is particularly sensitive to back-reflections from behind the antenna [12]; so, if the antenna cannot be placed directly against a non-reflecting surface, then it is usually best to put it as high above any background as practical (keeping in mind stability and access requirements). In any event, the space between the antenna phase centre and its backing surface should strictly avoid small multiples of the L-band half-wavelength within the near field of the antenna [13]. A clear view of the sky down to at least 10° elevation, preferably 5°, is needed in order to allow robust geodetic determinations of the antenna position.

There have been some poorly supported claims of strong variations of geodetic clock estimates with temperature changes in some GPS antennas, together with recommendations to use temperature-stabilized units. While this might apply to certain low-end, single-frequency units (or when using code data only), direct tests of a standard AOA Dorne Margolin choke ring antenna have failed to detect any sensitivity of the clock estimates to antenna temperature variations. Ray and Senior [14] placed an upper limit of 2 ps K<sup>-1</sup> on the short-term (diurnal) temperature sensitivity and later extended this to <10.1 ps K<sup>-1</sup> for any possible long-term component [5]. Even smaller sensitivities, 0.17 ps K<sup>-1</sup> or less, were determined by Rieck *et al* [15] for an Ashtech choke ring model.

As with the satellite transmitter antennas, and recognized much earlier, the beam patterns of GPS tracking antennas deviate from the perfectly hemispherical ideal [16]. Effectively, this means that the phase centre of the antenna, and hence the geodetic reference point, will depend on the direction of the signal from a particular satellite. Azimuthal variations have usually been ignored and only the elevation-angle dependence considered, although this is likely to change in the future. The IGS has developed sets of phase corrections to apply in the data analysis for each particular antenna model. Neglecting these effects can cause systematic errors in station height determinations up to ~10 cm. The present IGS approach uses differential phase corrections relative to the AOA Dorne Margolin T choke ring antenna as a standard reference, and most of the measured values follow the methodology of Mader [17], described at the website [www.ngs.noaa.gov/ANTCAL/](http://www.ngs.noaa.gov/ANTCAL/). The phase patterns of the satellite transmitters have been ignored. However, it is expected that the IGS will transition to using absolute antenna patterns for satellites and tracking stations [10], perhaps by the end of 2005.

Many permanent GPS antennas have been fitted with radomes for protection of the choke ring elements from filling

with snow or miscellaneous rubbish. These invariably affect the performance of the GPS system, mostly by distorting the wavefront phases, which can give rise to apparent shifts in station position, especially height. Differences in position, with and without a radome, can reach the level of several centimetres. Tests have shown that conical radomes are usually most problematic; some types of hemispherical radomes seem to show minimal effects. Currently the IGS does not account for the presence of radomes in its published antenna phase centre tables—all antennas are treated as radome-free even when phase centre corrections have been measured for the radomes. The best general advice is to avoid the use of radomes unless absolutely necessary. Otherwise, choose a hemispherical radome whose effect has been measured and found to be minor.

### 2.3. Antenna cables and connections

The cable run from the GPS antenna to the receiver should be as short as feasible and use a single continuous segment. No signal splitters or other components should be inserted in order to ensure the best possible power and impedance matching. While specific tests of the effects of splitters or other such elements on clock performance are very limited, anecdotal evidence indicates degradations whenever additions of this type have been made. (Rieck *et al* [15] report temperature sensitivity results, but did not study multi-path or other effects.) The connectors should be well sealed against moisture and exposure. The type of cable should be chosen to have good phase-stability properties, low temperature sensitivity (<0.1 ps K<sup>-1</sup> m<sup>-1</sup>), and low loss. Cable runs across open ground should be avoided in favour of a trenched conduit. Generally, any effort to reduce exposure to environmental influences is advisable.

### 2.4. GPS receivers

Geodetic GPS receivers must report pseudorange and carrier-phase observables at both the  $L_1$  and  $L_2$  frequencies. For time comparisons, the receiver must also have the ability to accept reference frequency and 1 pulse per second (PPS) inputs from an external standard and use them faithfully for its internal timing functions. (In principle, the receiver-lab timing offset can alternatively be determined from an output 1 PPS signal, rather than by inputting a steering 1 PPS, but such arrangements are not common.) Such features are often purchase options for otherwise standard geodetic equipment. At  $L_1$ , most receivers in the IGS network track the P1 code over the narrower C/A code, and so experience with C/A-only models is limited. No side-by-side comparisons of clock performance have been reported for the different types of code tracking. On the other hand, no discernible difference has been seen for the few models in common use [5]. The essential requirement is that the code multi-path susceptibility should be low.

Various studies have shown the detrimental effects of temperature variations on the frequency stability of GPS receivers [15, 18–21]. Typical sensitivities are of the order of  $\pm 100$  ps K<sup>-1</sup>, with large variations among individual units, even for the same model. Therefore, for high-performance time and frequency applications, it is essential that the GPS receiver equipment be maintained in an environmentally

controlled location, with thermal fluctuations preferably no greater than  $\sim 0.1$  K.

Many receivers have user-selectable settings for various functions such as enabling onboard code-smoothing or steering of the internal receiver clock to GPS Time. The latter setting must be disabled for useful time comparisons. It is also usually advisable to disable code-smoothing as this is better handled in the subsequent data analysis. Standard geodetic practice is to track all satellites in view (including those flagged unhealthy and at low elevations). If necessary, low-quality data can be edited in the analysis process.

As with any time and frequency distribution system, it is essential that the input reference frequency and 1 PPS signals be kept coherent with one another and well isolated from interference sources. Care should be taken especially with the generation of secondary input frequencies, if required. Furthermore, the 1 PPS ticks must usually be within some small tolerance of GPS Time, such as  $< 30$  ms, for the receiver to function properly.

GNSS observational data are universally transmitted using the RINEX (receiver independent exchange) format, which is described at <ftp://igsb.jpl.nasa.gov/igsb/data/format/rinex210.txt>. This document also contains format specifications for navigation messages, meteorological data and related information. Generally, it is advisable to archive the raw, native data files from the receiver, in addition to the RINEX files, in case a problem in the translation is discovered later. Timing users can derive the file types used for CV ('CGGTTS format') from RINEX files using a tool developed at the Royal Observatory of Belgium [22].

### 2.5. Evaluating multi-path effects and system testing

Once a geodetic station has been established, the data quality should be thoroughly assessed before it is made operational. If problems are found, they should be ameliorated as much as possible. The University Navstar Consortium (UNAVCO) has developed a very informative website ([www.unavco.org/facility/facility.html](http://www.unavco.org/facility/facility.html)), which contains helpful advice and test reports on equipment for continuously operating GPS stations. They also maintain a range of software tools. In particular, the 'teqc' toolset is indispensable for handling and examining raw GPS data, including RINEX file translation, data editing and quality checking [23]. Using teqc output, most fundamental problems with data quality can be spotted, such as excessive cycle slips, incomplete data capture, blockages in sky coverage and so forth. The teqc diagnostics MP1 and MP2 measure the RMS variations of the code multi-path at  $L_1$  and  $L_2$ , respectively, assuming that the effects of phase multi-path are negligible. An unknown bias is reset for each satellite pass, and so these multi-path metrics are insensitive to long-period signals that can be important for timing. Also, because of intrinsically different behaviour for different receiver types, the  $MP_i$  measures generally lack absolute meaning and cannot be compared easily from one site to another. However, unexpectedly large multi-path variations with elevation angle and over time can indicate site or configuration problems. In at least one case, MP2 variations were found to correlate strongly with changes in geodetic clock performance [5].

If PPP solutions (see below) can be generated for the receiver clock behaviour using precise orbit and satellite clock products from the IGS, then a code-only solution compared with code + phase can reveal unexpected problems with the pseudorange data. Another useful diagnostic is the level of discontinuities in clock estimates between consecutive 1 day analysis arcs [5], which mostly reflects variations in pseudorange multi-path noise (see below). Other methods of investigating multi-path errors—such as the sky distribution of post-fit residuals from a geodetic solution or high-frequency variations in GPS signal-to-noise ratios—usually focus on phase effects, rather than on the pseudorange. The classic test, though, is repetition of a particular error pattern from one day to the next at the nominal period of one sidereal day. In fact, due to operational details in the management of the GPS constellation, the repeat cycle of the satellite-ground geometry is closer to 23 h 55 min 55 s rather than the true sidereal period [24].

### 2.6. Calibration of tracking station delays

To compare clock readings at one station with those at another using any intervening system requires that the internal delays within all the instrumental hardware be accurately known. The process of doing so is known as calibration. Generally, we may consider two classes of calibration methods: absolute determinations, where an end-to-end set of bias measurements is made using a GPS signal simulator, which itself must have been accurately calibrated, and differential determinations, where a side-by-side comparison is made against another similar system taken as a standard reference. In practice, both methods are used. A small number of geodetic receivers have been calibrated in an absolute mode. These are then used as travelling standards to differentially calibrate a much larger number of receivers deployed operationally [25].

Presently, only one geodetic GPS receiver type has been calibrated absolutely, the Ashtech Z-XII3T, using a simulator facility at the US Naval Research Laboratory [6, 26, 27]. The absolute results agree within their reported uncertainties of about 3.5 ns with a differential measurement relative to a previously calibrated classical CV timing receiver [28]. The dominant error source in the absolute calibration procedure is thought to be the GPS simulator itself [27]. Subsequent differential calibrations against an absolute standard can be made with smaller uncertainties of about 1.6 ns (Petit, private communication), but the long-term stability of such measurements is still open to question.

For the convenience of users, the GPS data from a calibrated receiver can be adjusted to remove the instrumental bias in the process of generating RINEX exchange files. The specified manner of doing this is to write the clock offset correction,  $dT$ , into a field reserved on each observation epoch record and modify the reported observables according to the following relations in order to maintain their strict consistency:

$$\text{Time(corrected)} = \text{Time} - dT,$$

$$\text{PR(corrected)} = \text{PR} - (dT \times c),$$

$$\text{Phase(corrected)} = \text{phase} - (dT \times \text{freq}),$$

where ‘Time’ is the observation epoch, ‘PR’ is the pseudorange and ‘phase’ is the carrier phase for frequency ‘freq’. Providing the clock offset correction value for each observation epoch allows the reconstruction of the original observations, if necessary. However, this RINEX feature is limited by the format specification to clock offset values truncated to the nearest nanosecond. If sub-nanosecond clock calibration corrections are applied without using the RINEX clock offset field, then the clock correction value should be documented as a comment in the RINEX file header.

### 3. Data analysis strategies

The recognition that GPS could be utilized to achieve geodetic accuracies several orders of magnitude better than was originally conceived is usually attributed to Counselman and Shapiro [29]. Applying astronomical techniques developed for very long baseline interferometry (VLBI), they proposed using the carrier phase as the main GPS observable rather than the pseudorange. By very precise tracking of changes in the GPS signal phase it was shown how relative position determinations could be made to the centimetre level rather than to tens of metres. Soon afterwards, Bossler *et al* [30] introduced an innovative double-differencing method to aid in resolving the integer phase ambiguities of the carrier signal. Developments followed quickly thereafter, drawing heavily on the heritage of VLBI methods and models, most of which apply directly to GPS as well. The main analysis differences are the additional orbit-related parameters of GPS and the relative weights of the group delay observables (vital for VLBI, not for GPS except for clock solutions) and the phase observables (vital for GPS; usually included only as low-weight time derivatives in VLBI).

#### 3.1. GPS observation equation

The basic steps for reducing GPS observations are outlined in ICD-GPS-200 and many succeeding publications. For a given satellite and tracking station pair, the pseudorange observation equation for each observing frequency,  $i$ , can be written as

$$P_i = R + c(C_r - C_s) + I_i + T + e_i \quad (i = 1, 2),$$

where  $i = 1, 2$  correspond to the two frequencies  $L_1$  and  $L_2$ ,  $c$  is the vacuum speed of light,  $C_r$  is the clock synchronization offset of the tracking station at the time of signal reception (including all internal delay components),  $C_s$  is the clock offset of the transmitting satellite at the time of emission,  $R$  is the distance traversed between the satellite phase centre emission and receiver phase centre reception,  $I_i$  is the ionospheric delay,  $T$  is the delay due to the neutral atmosphere (mostly troposphere) and  $e_i$  is the measurement error (including both thermal noise and such other sources as multi-path). Thermal noise in the antenna and receiver places a theoretical lower limit on the size of the measurement errors, which depends to some extent on the particular tracking technology employed by the receiver. Zero baseline experiments, where most external effects such as multi-path can be removed, show the RMS of the C/A pseudorange and the L1 carrier phase measurement noises to be 4 cm and 0.2 mm, respectively, for a pair of Ashtech Z-12 receivers [7]. However, local environmental

effects always dominate actual measurement noise. Standard *a priori* values for geodetic processing are around 1 m and 1 cm for the pseudorange and carrier phase and errors, respectively, based on observed post-fit residuals [3, 31].

The ionosphere is dispersive (delay approximately proportional to the inverse of the frequency squared) and is opposite in sign for pseudorange and phase. The linear combination of the two frequencies

$$P3 = 2.5457 \times P1 - 1.5457 \times P2$$

is, to first order, free of ionospheric effects (see [32] for a study of the second-order effect). So,

$$P3 = R + c(C_r - C_s) + T + e,$$

where  $e$  is the combined error of  $P1$  and  $P2$ . The observation equation for phase observables is the same (expressed in distance units) with the addition of an ambiguity term ( $N_i \cdot \lambda_i$ ) for the unknown number of phase cycles at each carrier frequency. It is apparent that the ambiguity parameters,  $N_i$ , are formally indistinguishable from the clock offset parameters when using only phase data. In principle, if the clock offsets are fixed to some arbitrary values, then their subsequent variations can be tracked, which means that phase-only solutions can provide useful frequency, but not timing, comparisons. More commonly (and the case of interest here), simultaneous code data are combined with phases to permit both clocks and ambiguities to be estimated, where only the code observations contribute to the average clock offsets. In a secondary process, confidently determined ambiguity parameters can be ‘fixed’ (or tightly constrained) to integer values. Doing so for a large fraction of the ambiguities greatly strengthens the overall geodetic solution and reduces parameter correlations. However, ambiguity fixing is only practical on the basis of double-difference observations because the various satellite and receiver biases would not allow a reliable choice of the proper integer value for undifferenced data.

The range,  $R$ , is given in terms of the geocentric coordinates of the satellite ( $X, Y, Z$ ) and the receiver ( $x, y, z$ ) antenna phase centres by

$$R = \sqrt{(X - x)^2 + (Y - y)^2 + (Z - z)^2}.$$

When using coordinates for the satellite centre of mass or receiver geodetic marker, rather than phase centres, appropriate eccentricities must be applied based on external measurements. The solved-for clock estimates refer to the antenna phase centres regardless of any coordinate eccentricities. The GPS broadcast message provides values for each satellite position (phase centre) and clock reading as a function of time, accurate to a few metres. With simultaneous observations of at least four different satellites and a crude model for the tropospheric delay, the position and clock reading for a user receiver can be determined to <10 m at each epoch. If the user position is known *a priori* and only the clock is unknown, then just one satellite pseudorange observation is needed.

Common-view clock comparisons are made by differencing simultaneous data from two receivers with known coordinates. Then the effect of satellite clock error is removed, together with much of the satellite position error

and tropospheric delay. For conventional CV measurements, using only single-frequency C/A pseudoranges, ionospheric modelling errors usually limit the accuracy of the determinations of remote clock differences. This can be significantly improved using the linear combination of codeless P1 and P2 observations, as is done in the P3 CV method [22]. As a rule, the accuracy of CV clock comparisons worsens with increasing distance between the receivers because the common-mode cancellation of the neglected terms becomes progressively less effective. To attenuate these effects, the CV method for UTC has been modified in recent years. Precise orbit corrections have been applied since the early 1990s for very long baselines, and corrections computed from the highly accurate IGS orbits and ionosphere maps (see [igsceb.jpl.nasa.gov](http://igsceb.jpl.nasa.gov)) have been used since 2001 (Petit, private communication). Further refinements can be made, such as better tropospheric modelling and accounting for geophysical motions (e.g. tidal displacements). Such incremental modifications, however, fail to take advantage of the inherent precision of the phase observables, and so the CV timing results cannot reach the level of the full geodetic technique, particularly over intervals less than 1 day or so.

In geodetic analyses, the broadcast navigation information is not used except possibly for the first level of data screening and editing. The highest quality *a priori* models are evaluated for all known geophysical effects and the remaining unknowns are adjusted from the data using physically plausible parametrizations. In most cases, it is advantageous to fix the satellite clock and orbit values to the very accurate determinations published by the IGS since the general GPS user is unlikely to do as well. This greatly simplifies the estimation of receiver clocks, provided the IGS conventions and models are also strictly followed.

### 3.2. Methods for global solutions

In the case where satellite clocks and orbits are to be determined, rather than taken from an external source, we first consider procedures like those used by the IGS analysis centres, where data from a global tracking network are reduced in large simultaneous adjustments. A globally well-distributed network of receivers is required to determine satellite orbits and clocks. Analysis arcs are usually segmented into 24 h batches, coinciding with the standard RINEX daily files that normally contain observations from 00:00:00 to 23:59:30. (Note that the IGS convention uses GPS Time for time tags in all its data files.) For some solution types, multi-day analysis arcs may be formed by linking together several successive one-day arcs. The initial processing step involves screening the data files from each station. It is necessary to check and edit for potential problem data, repair or flag slips in the carrier phases, adjust for small time tag drifts in some receiver types and correct for pseudorange biases in cases where P1 and P2 are not available. The screened data are generally reformatted into direct access files appropriate to the chosen analysis system.

All geodetic adjustment methods assume the availability of sufficiently accurate *a priori* information that parameter estimation is linear and thus generalized least-squares methods can be applied. The broadcast navigation message can be used if no better sources are at hand. If necessary, such as

for a new station, solution iteration may be used to satisfy the linearity condition. The *a priori* satellite orbits are rotated from an Earth crust-fixed frame (used for orbits distributed in the broadcast message as well as by the IGS) to an Earth-centred inertial (ECI) frame using an assumed set of Earth orientation parameter (EOP) values. Typically, the EOPs are those produced by the IGS or by the International Earth Rotation and Reference Systems Service (IERS); see their website at [www.iers.org](http://www.iers.org). In the ECI frame, the satellite orbits can be fitted to parametrized models for the dynamical motions and integrated. This step is needed to generate parameter partial derivatives if the orbits will be adjusted in the following data fitting. Various forms have been developed to describe GPS satellite motions, from the finite-element approach of Fliegel *et al* [33] to the empirical model of Beutler *et al* [34]. Even though a better physical model of the behaviour of the satellites would be expected to be superior to a purely empirical approach, experience suggests that any gain is negligible. This is because, for high-accuracy geodetic applications, the orbit parametrization must be intense enough to capture centimetre-level motions, which is exceedingly difficult to accomplish for real satellites without using at least some empirical parameters. The motions are complicated by variations in acceleration as the exposure to solar radiation pressure changes and especially by micro-thrusting events that are used to maintain the attitude of some older satellites.

The observation equation is evaluated for each data point, using the *a priori* station coordinates also rotated to the ECI frame. In addition to the basic effects already mentioned, contributions due to a number of smaller effects must also be included (see next section). The parameters are adjusted to fit the observations by minimizing the residuals using standard methods, such as batch least-squares, sequential least-squares or a Kalman filter. Kalman and related filters are particularly adept at handling clock parameters as they easily accommodate stochastic noise processes appropriate for realistic clock variations. For a global network of some tens of tracking stations, the full set of parameters that are usually adjusted includes the following: up to three geocentric coordinates for each station (subject to some specification of the terrestrial datum, such as constraints on the positions of certain reference stations); time-varying receiver clock parameters (which must be sufficient to allow nearly arbitrarily large variations from epoch to epoch); orbital parameters for each satellite (at least the six Keplerian elements, or equivalent, plus a Y-bias and other empirical terms); time-varying satellite clocks; time-varying zenith tropospheric delays (as well as possible azimuthal gradients); EOP offsets and rates for polar motion and length of day; and carrier-phase ambiguities. Sometimes, additional minor parameters are included for effects such as variations in satellite attitude or net offsets in the tracking network origin from the Earth's centre of mass. The set of clock parameters has a rank deficiency of one since there is no absolute information for any clock epoch. Standard geodetic analyses resolve the defect by choosing one specific clock (usually a very stable ground clock) to be unadjusted as a reference in the estimation process. Estimates of all other clocks are then determined relative to that fixed clock. Alternatively, the clock datum can be specified by fixing a linear combination of the available clock offsets to be equal to

zero (or any specified value, such as GPS Time). The relative clock differences among all station pairs are unaffected by the choice of the reference datum.

For the highest quality results, ‘fixing’ of at least some of the phase ambiguity parameters is desirable. Because of the huge difficulty in attempting to do this with undifferenced one-way observations, the normal procedure is to apply tight constraints on the integer values of double-differenced ambiguities for selected station pairs. Successfully doing so for a major fraction of the ambiguity parameters greatly stabilizes the overall solution. In most cases, iteration of the solution can increase the number of ambiguity parameters successfully fixed and improve the data editing.

### 3.3. Reference frames and models for correction terms

In evaluating the basic GPS observation equation, a number of minor effects must also be considered if centimetre-level results are expected. Most of these are documented in the IERS conventions [35]. The geocentric coordinate system used for points attached to the Earth’s surface is the International Terrestrial Reference Frame (ITRF) [36]. Transformation from ITRF to the ECI frame takes into account movements of the pole in the Earth frame and rotation about the pole. Movement of the pole in inertial space (i.e. nutation; see [35]) is sometimes neglected or handled only approximately as near-Earth satellites are not very sensitive to this effect. So the ECI frame is not always precisely aligned to the International Celestial Reference Frame (ICRF), a nearly inertial system formed by the VLBI positions of extragalactic radio sources and whose origin is the solar system barycenter.

The correction terms for the satellites are the offsets described previously, between the centres of mass and the antenna phase centres, and the phase rotation of the signal polarization due to changes in perspective. The latter effect, known as ‘phase wind-up’ or in astronomy as parallactic angle, arises because the GPS signal is right circularly polarized. As the viewing geometry between the receiver and satellite varies, the polarization phase appears to change correspondingly. A correction must be applied in evaluating the carrier-phase observations, but not the pseudoranges, as described by Wu *et al* [37].

The receiver position corrections are much more diverse and complex due to geophysical effects [35]. The mostly vertical motions of surface points due to the solid Earth (‘body’) tide have amplitudes of a few decimetres at mid-latitudes and must be accurately modelled. The corresponding motions of the crust due to ocean tidal loading are nearly an order of magnitude smaller at most places but can be amplified in some coastal areas. If estimating the GPS orbits, then the variations in the geopotential due to the solid Earth and ocean tides should also be included in the *a priori* orbital integrations. The pole tide correction accounts for large-scale rotational deformation due to variations in the pole’s position with respect to the Earth’s crust. The polar motion itself and the rate of rotation undergo rather large diurnal and semidiurnal modulations due to tidal motions of the ocean. When the GPS satellites are expressed in an inertial frame, corrections for these large-scale motions of the Earth frame should be applied. The IGS orbits, in an Earth-fixed frame,

have already included the sub-daily EOP variations and so there is no net effect for a terrestrial observer. Accurate models for all these effects have been given by McCarthy and Petit [35]. In addition, users should apply the antenna-specific phase-centre corrections recommended by the IGS and described previously.

Even though international scientific unions advocate the use of Geocentric Coordinate Time (TCG) for the analysis of near-Earth satellite data, most (if not all) analysis groups continue to use Terrestrial Time (TT). TT differs from UTC and TAI only by an offset, whereas TCG differs in rate (frequency) from the other scales due to general relativistic effects. Consequently, the clock frequencies from the IGS and other GPS analysis groups should be directly comparable with those measured in timing laboratories. Some physical constants, such as the gravitational constant–Earth mass product,  $GM$ , depend on the choice of relativistic reference frame and so care should be taken to use the appropriate values.

Three types of relativistic correction are usually applied in GPS processing; see also Kouba [38] for further details. (1) The first-order frequency shift, relative to TT, due to time dilation and gravitational potential difference has already been applied in the GPS system by setting oscillator offsets in the spacecraft, assuming nominal orbital elements. The second-order correction for non-circular GPS orbits must be applied by the user; see ICD-GPS-200. (2) A ‘dynamical’ correction to the acceleration of near-Earth satellites is given in the IERS conventions [35]. (3) The coordinate time of propagation, including the gravitational delay, is given separately in the IERS conventions (but is often neglected).

### 3.4. Precise point positioning

Rather than form large global network GPS solutions, for most applications it is much more economical and efficient to analyse data from individual stations in the PPP mode [3]. In this approach, accurate satellite orbits and clocks are taken from some prior source and applied without adjustment. (In some variations of the PPP method, partial relaxation of the orbits and clocks is permitted.) Applying all the same models as discussed above, the user can determine coordinates, clock variations and tropospheric delays for an isolated, single receiver [39]. The quality of the results will depend directly on the accuracy and consistency of the assumed satellite information. The reference frame and datum of the assumed orbits and clocks will be inherited by the PPP results and so it is important that these be well defined and stable. The IGS products (see below) are expressly intended for this purpose. Kouba [40] provides a guide to the proper use of IGS products for PPP analyses. For 1 day solution arcs, typical position repeatabilities should be at the level of about 10 mm in the vertical and 3 mm to 5 mm in the horizontal. The PPP receiver clock results should be precise to a similar level, <100 ps, but the accuracy (not including the calibration uncertainty) will normally be poorer (see below); the PPP timescale will be that of the *a priori* satellite clocks.

### 3.5. Effects of errors on clock solutions

Errors in the analysis models, *a priori* information or observational data will influence GPS clock estimates. Dach *et al* [41] have used simulations to examine the signatures of

various types of input error. For instance, a station height error will cause a frequency offset for long east–west baselines. In the time domain, a discontinuity is introduced at the boundary between processing arcs due to this error. Satellite orbit errors can have similar effects. In actual practice, these error effects are not likely to be very significant in IGS products since station and satellite positions are adjusted together with the clocks. Probably more important is the confirmation by Dach *et al* that pseudorange noise at the 0.5 m level, even if assumed to have a white noise distribution, will cause offsets between discrete 1 day processing arcs at the levels seen in actual clock results (see more below). Coloured pseudorange noise (e.g. from multi-path or temperature dependences) presumably has an even more pronounced effect on clock jumps between arcs.

Using more pseudorange data (higher sampling rate and/or longer arcs) would be expected to improve the clock accuracy. Higher sampling rates will only be effective as long as the dominant multi-path wavelength is shorter than the sampling period; otherwise the clock errors will not average down with the addition of more data. As shown by Senior *et al* [42] for the clock formal uncertainties, longer analysis arcs should average down the code noise effects, although less effectively than  $\sqrt{N}$ . However, this has not been demonstrated for actual clock results, only for their formal errors. It has also not been determined whether longer arcs differ only by a net clock bias or whether the frequency content is also changed (improved). If longer arcs provide better clock accuracy only in a bias sense, then other analysis approaches should give nearly equivalent results, such as a suitable post-analysis filtering of shorter-arc results. The latter approaches could prove more economical or better suited for some applications.

Discontinuities between independent analysis arcs are natural and expected for all geodetic parameters, including orbits, tropospheric delays and clocks. The offsets should reflect the inherent quality of the GPS data and analysis methods. The magnitude of clock jumps tends to be larger than for most other parameters because only code data contribute, though effectively averaged over the analysis arc. Various approaches have been considered to minimize the day-boundary clock discontinuities. The obvious method would be to avoid discrete analysis batches altogether and to use some type of continuous processing scheme [42, 43]. However, this is difficult to accomplish in practice and can cause some error effects to accumulate [41]. Long analysis arcs will also cause clock estimates to be correlated over the same periods (random walk type statistics), which could limit the stability that might otherwise be obtained using independent analysis arcs (white noise behaviour). An alternative method of removing analysis discontinuities is to concatenate time series using overlapping arcs to determine the offsets (e.g. [44, 45]). Even if the clock jumps at arc boundaries obey a white noise distribution [5], the effect on the concatenated series will be the addition of a random walk noise component. In other words, the concatenation process also causes long-term clock correlations and could limit the long-term stability that might otherwise obtain. Dach *et al* [46] consider other more sophisticated methods of generating nearly continuous clock results within the estimation process itself by passing information from one arc to the next. These act much like a filter/smoothener to improve the short-term time transfer stability with little effect at longer intervals.

It is difficult to understand the widespread efforts to suppress clock jumps at arc boundaries, especially when they are small (at the 100 ps to 200 ps level). As with any real measurement process, a non-zero error is inevitable. A valid interpretation of the geodetic clock measurements can only be made based on a reasonable understanding of those errors. Using suppression methods that introduce long-term correlations into the clock time series (such as by concatenation) would seem to be particularly counterproductive. If elimination of the discontinuities is genuinely needed, then a filter/smoothener method is probably preferable to avoid the problem of correlated time series, although this can distort the short-term clock behaviour. On the other hand, the discontinuities themselves provide valuable diagnostic information on the quality of the station installation (see below). If the jumps are larger than the standard noise level of about 120 ps [5], then the underlying causes should be identified and ameliorated, not hidden from view by post-analysis manipulations.

#### 4. IGS clock products and timescales

From its inception in 1994, the IGS has provided daily files of accurate satellite positions and clock readings, tabulated at 15 min intervals. Since then, new or modified products have been added from time to time. All IGS products (see <http://igsb.jpl.nasa.gov/components/prods.html>) are formed by the weighted averaging of solutions submitted by up to eight contributing analysis centres. While the data sets used by the individual groups usually overlap, the effects of differing analysis strategies, modelling and software are largely independent. So, properly weighted combinations of the individual results are generally superior to any single solution. In this way, the IGS products probably benefit in precision and accuracy, but certainly in stability, reliability and robustness, compared with the results of any individual analysis group.

##### 4.1. Available product sets

The IGS ‘classical’ clock products were changed on 5 November 2000 (GPS Week 1087) when a new combination algorithm was implemented and the clock products were expanded to include many of the receivers in the tracking network, as well as the satellites [47]. The tabulation interval of the new clocks (satellites and tracking stations) was reduced to 5 min, compared with the prior 15 min sampling of the satellite clocks. Three series of product lines are generated based on data latency: (1) the Ultra-Rapid products (with satellite clocks but not receivers), which are intended for real-time users by publishing 24 h predictions; (2) Rapid products, released about 17 h after the end of each day; and (3) the definitive Final products, released about 13 days after the end of each week. Table 1 summarizes the IGS orbit and clock products, latencies and estimated accuracies. (In addition to those shown in the table, the IGS provides ionospheric maps, tropospheric zenith path delays, EOPs and so forth.) All products are available from the IGS data centres or Central Bureau; see [igsb.jpl.nasa.gov](http://igsb.jpl.nasa.gov). Use of the IGS Rapid or Final products instead of broadcast information allows PPP determinations at the 1 cm level for 24 h arcs.

**Table 1.** IGS combined orbit and clock products and their characteristics compared with broadcast values. Orbit accuracy estimates, except for predicted orbits, are based on comparisons with independent laser ranging results. Precisions are better than the quoted accuracies. Product files are for 24 h periods except that the Ultra-Rapids span 48 h. The 5 min clock data are available in ‘clock RINEX’ format files, while 15 min clock samples are available in SP3 format files together with the satellite ephemerides.

GPS satellite ephemerides and satellite/station clocks		Accuracy estimates	Latency	Update intervals	Sample interval
Broadcast	Orbits	~200 cm	Real time	—	Daily
	Sat. clocks	~7 ns			
Ultra-Rapid (predicted half)	Orbits	~10 cm	Real time	Four times daily	15 min
	Sat. clocks	~5 ns			
Ultra-Rapid (observed half)	Orbits	<5 cm	3 h	Four times daily	15 min
	Sat. clocks	~0.2 ns			
Rapid	Orbits	<5 cm	17 h	Daily	15 min
	Sat. & stn. clocks	~0.1 ns			5 min
Final	Orbits	<5 cm	~13 days	Weekly	15 min
	Sat. & stn. clocks	~0.1 ns			5 min

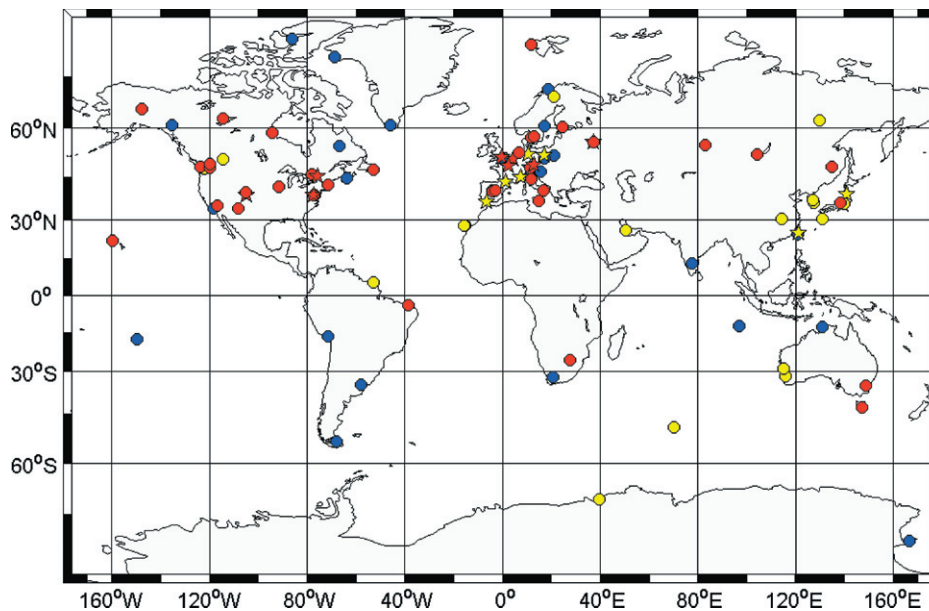


**Figure 1.** Map showing distribution of IGS stations using external frequency standards (as of November 2004). Colours indicate the type of standard: red are H-masers, yellow are caesiums and blue are rubidiums. IGS stations co-located at timing labs are indicated by star symbols.

The IGS tracking network consists of more than 350 globally distributed receiver installations. All stations operate continuously and report daily (at least) RINEX observation files with 30 s samples. Most of the stations use internal crystal oscillators, which are steered by their own observations to track GPS Time, but more than 100 IGS stations are equipped with external frequency standards. Figure 1 shows the distribution and type of external standards within the IGS network (as of November 2004). About 51 use H-maser standards, 28 use Cs clocks and 27 use Rb clocks. A subset of these, about 20, are co-located at timing labs.

4.2. IGS timescales

There is no specific requirement for the underlying timescale of the clock products when used for geodetic positioning applications, except that it should be reasonably close to GPS Time. An important strength of GPS geodesy is that it does not depend, to first order, on the stability or accuracy

of the timescale since the effects of clocks can be removed by double differencing. Nonetheless, it is desirable for the reference timescale to possess other properties, such as being highly stable and accurately traceable to UTC. These qualities enhance the value of the IGS clock products for applications other than pure geodesy, especially for timing operations.

The IGS originally used as a reference for its clock products a simple daily linear alignment of the observed satellite clocks to broadcast GPS Time. However, the instability of GPS Time is comparatively large, about  $2 \times 10^{-14}$  at 1 day, which is at least an order of magnitude poorer than the instability of the best frequency standards in the IGS network. Even some of the newer Block IIR satellites have clocks that are more stable than the ensemble GPS Time due, in part, to the bang-bang steering algorithm used to keep the broadcast timescale aligned to UTC (via the realization maintained by the US Naval Observatory). The old IGS procedure of aligning its clocks each day to GPS Time introduced large day-to-day discontinuities in both time and frequency (see figure 2). There

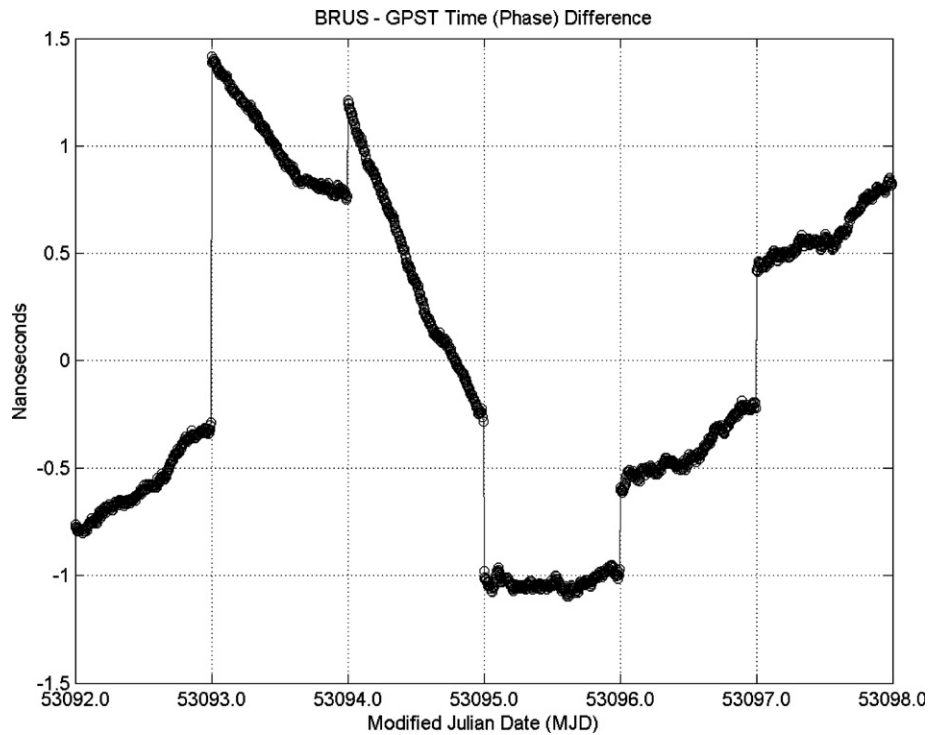


**Figure 2.** GPS geodetic time transfer estimates from the IGS Final products for the BRUS station in Brussels, during the period 28 March through 2 April 2004. The timescale is fixed by a daily linear alignment to GPS Time. The BRUS instability is dominated by this timescale choice, which is responsible for the large discontinuities in time and in frequency. A linear trend has been removed for plotting.

is no impact of this procedure on the usefulness of the products for precise positioning, but the utility for time and frequency dissemination is certainly limited.

To improve the instability of the Rapid and Final clock products, new IGS internal timescales were developed. The new timescales are formed as weighted ensembles of the included clocks, for both stations and satellites. A detailed description of the algorithm is given by Senior *et al* [48]. Each timescale ('IGRT' for the Rapids and 'IGST' for the Finals) is driven largely by the available H-masers, though lesser clocks can contribute slightly, including the rubidium clocks onboard the Block IIR satellites. The algorithm is a Kalman filter implementation with a simple polynomial model for each clock followed by a linear quadratic Gaussian (LQG) algorithm for loosely steering the timescales to GPS Time. Weights for each clock are determined iteratively and dynamically based on the observed instability at several averaging intervals less than 1 day. An upper limit of weights is imposed for each clock to avoid the situation of a single clock overtaking the timescales [49]. The LQG steering algorithm is critically damped with a time constant of about 30–40 days. The results are timescales with instability generally better than about  $1 \times 10^{-15}$  at 1 day, but still limited in the medium and longer terms by the steering to GPS Time. There are periods, however, when the instability of the timescales can be degraded somewhat, such as when the number of H-maser stations in the clock products is unusually small.

Figure 3 shows the performance of the BRUS clock after changing the reference to the IGS Finals timescale, IGST. The inter-station clock information is the same as in figure 2; only the underlying timescales are different. The much improved

stability using the IGS timescale is evident. The remaining small discontinuities at some day boundaries reflect mostly the local BRUS data quality (see more below). It is possible that some effects of individual clocks, including day-boundary jumps, can adversely affect the ensemble timescales, due for instance to undetected data editing problems. However, evidence indicates that any such limitations are minor and that the ensemble timescales are far superior to any single contributing clock. The new IGS timescales were implemented in the official products in early March 2004 (see IGS Mail #4875 at [igscb.jpl.nasa.gov](mailto:igscb.jpl.nasa.gov)). Clock products aligned to the same internal timescales are available from November 2000 at the website <https://goby.nrl.navy.mil/IGStime>.

The long-term variation of each IGS timescale is illustrated in figure 4 relative to GPS Time and to UTC (approximately). Though the sub-daily to daily instability of the IGS timescales is greatly improved over GPS Time, the longer-term instability is similar owing to the continued reliance on GPS Time. Efforts are under way to tie the IGS timescales to UTC more accurately by using data from the BIPM and taking advantage of IGS stations co-located at timing laboratories [50].

## 5. Evaluation of performance by day-boundary discontinuity analysis

The 'absolute' accuracy of GPS-based clock estimates (modulo the calibration bias) is determined entirely by the pseudorange data, averaged over the analysis interval, usually 24 h. When analysing 1 day arcs of global data sampled at 5 min intervals, the formal error estimates for the

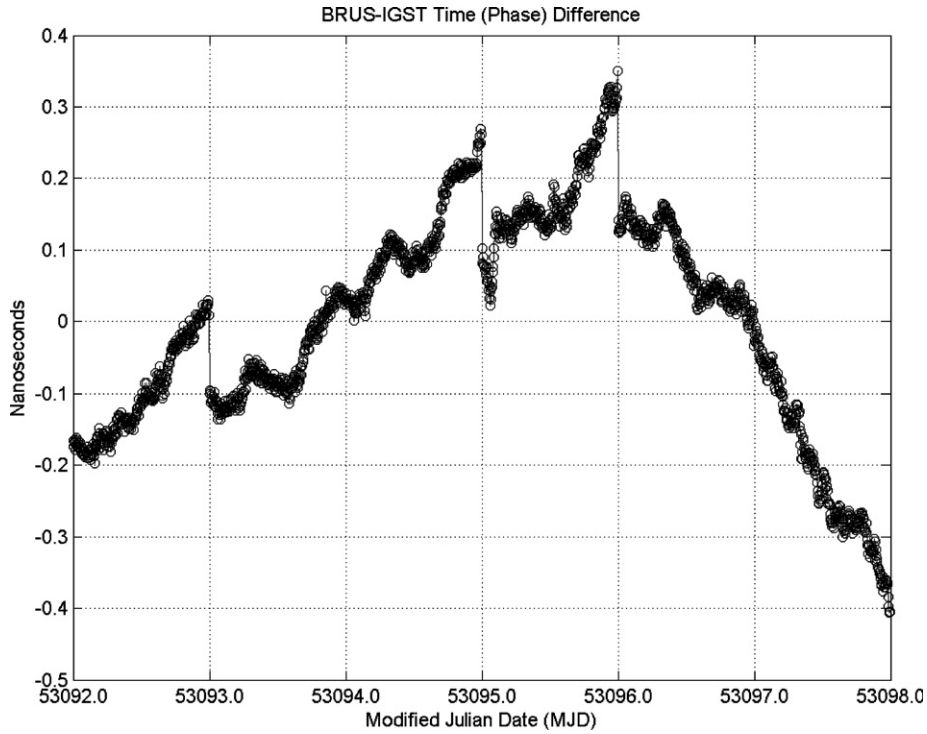


**Figure 3.** Same BRUS clock data as shown in figure 2 except referenced to the IGS Final clock timescale, IGST. A linear trend has been removed for plotting.

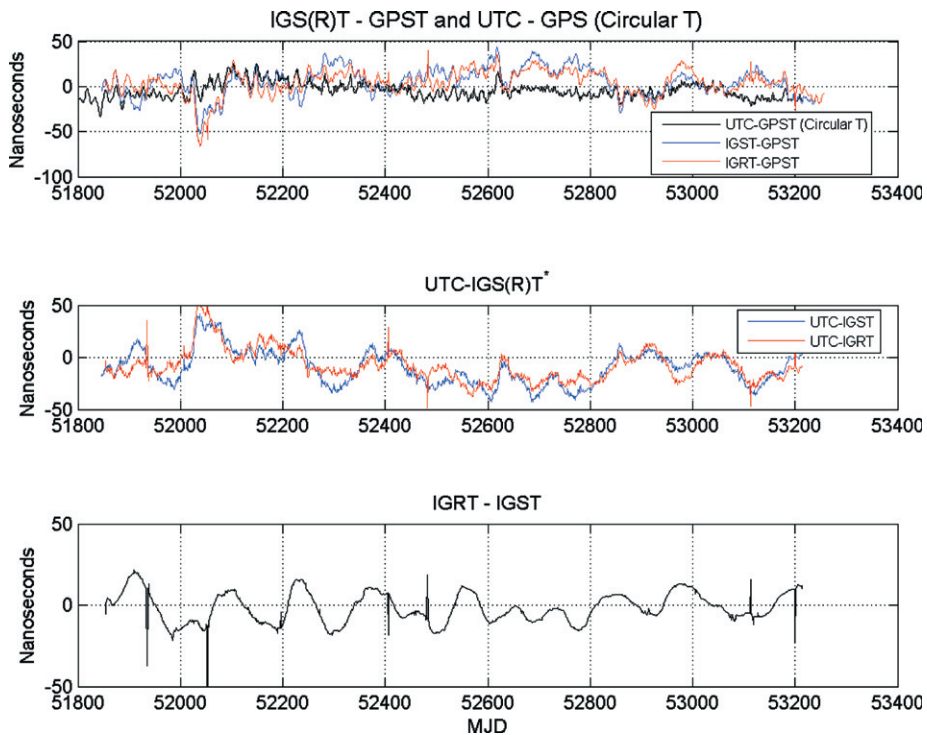


**Figure 4.** Comparison of the IGS timescales IGST and IGRT against GPS Time (GPST) and against UTC (modulo leap seconds) from 5 November 2000 through 28 June 2004. The top plot shows UTC minus GPST from the BIPM *Circular T* series as well as the IGS timescales IGST and IGRT minus GPST. The IGS and BIPM realizations of GPST can differ by several nanoseconds due to distinct observational and analysis strategies [50]. The middle plot shows UTC-IGST and UTC-IGRT obtained by differencing the time series in the top plot, which assumes that GPST is equivalent from *Circular T* and the IGS. Deviations from this assumption are responsible for a small portion of the plotted differences, especially at high frequencies. Finally, the bottom plot shows IGRT minus IGST, assuming each observes GPST equivalently. The occasional spikes are due to infrequent misalignment errors of the IGS Rapid clocks to GPST and are not actually present in either timescale.

clocks are typically about 120 ps, assuming each pseudorange observation has an uncertainty of 1 m. A more realistic test of actual measurement accuracy can be made by comparing clock estimates at the boundaries between independent analysis arcs for receivers equipped with very stable oscillators. (Less stable clocks can also be tested if overlapping analysis arcs are used to eliminate interpolation errors, but the adjacent clock estimates will then no longer be independent.) This is analogous to the classic geodetic repeatability test for a time series of position determinations.

Day-boundary clock jumps can be analysed for baseline solutions or for networks where a single station clock has been held fixed as the reference. The results can be difficult to interpret, however, since effects at two stations will be convolved in each clock time series. A superior approach is to use the IGS clock products, with the new highly stable ensemble timescale, for such an analysis [5]. By using station clocks aligned to the IGS timescales instead of clock pairs, it is possible to isolate observed behaviours to individual stations. Figure 5 shows an example of simultaneous time series of IGS clock estimates for nine H-maser stations. Note that the variability in the discontinuities among stations is independent of the stability of the individual clocks as some sites show large jumps but very good sub-daily stability and vice versa. The distributions for day-boundary offsets studied by Ray and Senior [5] were found to be zero-mean and Gaussian, but with RMS variations being highly site-specific.

The previous analysis of IGS clock jumps has been updated and extended in table 2. A total of 1310 days between October 2000 and June 2004 were examined from the IGS Rapid and Final clocks. The editing and processing criteria were the same as in Ray and Senior [5]. The maximum data gap at the day boundary is 30 min (typically 5 min), and so the interpolation noise due to instabilities in the H-maser standards should be negligible. Since the RMS statistics are for the differences between pairs of independent days, each daily accuracy estimate should be smaller by  $\sqrt{2}$ . Of particular note is the very large dispersion in RMS performance among stations, nearly one order of magnitude. This presumably reflects the wide range in code performance among these stations and, in turn, shows the vast variation in multi-path environments, external to the antenna as well as internal to the GPS instrumentation. In some cases the performance has varied markedly with time, sometimes correlated with changes reported in the site logs. Seasonal variations are found in a few cases. The RMS variations were previously shown to be independent of the choice of receiver or antenna model or the use of radomes.

The best long-term performance among the IGS stations studied is at ONSA (Onsala, Sweden), corresponding to a daily clock accuracy of  $(149 \text{ ps}/\sqrt{2}) = 105 \text{ ps}$ . BREW (Brewster, WA, USA), OPMT (Paris, France), BRUS (Brussels, Belgium), MAD2 (Madrid, Spain), WTZR (Wetzell, Germany) and GODE (Greenbelt, MD, USA) have only slightly larger daily clock errors, from 107 ps to 145 ps. There is a continuous progression of poorer performance among the other stations, up to 620 ps to 753 ps for ALGO (Algonquin, ON, Canada), NRC1 (Ottawa, ON, Canada) and METS (Metsahovi, Finland). The order of magnitude range of clock accuracy reflects variations in local conditions, not an

**Table 2.** Summary of day-boundary clock discontinuity statistics for 38 IGS stations with H-maser frequency standards. IGS Rapid and Final clocks from October 2000 till June 2004 were used. Stations co-located at timing laboratories are indicated by (TL).

IGS site	RMS clock jump/ps	Remarks
ONSA	149	Excellent
BREW	152	Excellent
OPMT (TL)	158	New station, so very limited data
BRUS (TL)	165	After changes in summer 2003 improved to 118 ps
MAD2	170	Very limited data, so RMS is not reliable
WTZR (TL)	189	
GODE	205	
USN1 (TL)	225	Station replaced by USN3 in July 2004
WSRT	227	Slight degradation since summer 2003
KHAJ	233	Limited data
CRO1	236	Maser no longer used
USUD	266	Maser no longer used
NPLD (TL)	268	
TID*	269	Appears improved since summer 2003
YEBE	271	
GOL2	271	Very limited data, so RMS is not reliable
AMC2 (TL)	283	Improved after antenna/receiver changes in June 2002
SPT0 (TL)	286	
WES2	296	
PIE1	305	Improved since receiver change in October 2002
STJO	334	
USNO (TL)	354	Appears worse since spring 2003
IRKT	359	
NYAL	363	Much better than NYA1 in 2004
NLIB	368	
MATE	389	Significant time variations; better in 2004
KOKB	460	Large degradation before antenna/cable change in May 2004
FAIR	478	Somewhat improved since summer 2003
DRAO	522	
YELL	564	Large seasonal variations, much worse in winters
ALBH	587	After September 2003 greatly improved to 97 ps
HOB2	631	Variations correlated with station changes
MEDI	703	
FORT	706	
NYA1	750	Large degradation since summer 2003
ALGO	877	Large seasonal variations, much worse in winters
NRC1 (TL)	936	Large seasonal variations, much worse in winters
METS	1065	Maser no longer used

artefact of the IGS timescale, for instance. Strongly supporting this conclusion are the temporal changes in performance seen at a number of stations. Abrupt changes usually correspond to known changes in configuration or equipment. (Regrettably, not all station changes are publicly reported.) A few stations show large seasonal variations, especially the three Canadian stations at YELL, ALGO and NRC1 (see figure 6). We previously speculated that the large increase in clock jumps during wintertime at these sites is caused by a buildup of snow and ice on surfaces below and in the near field of the antennas.

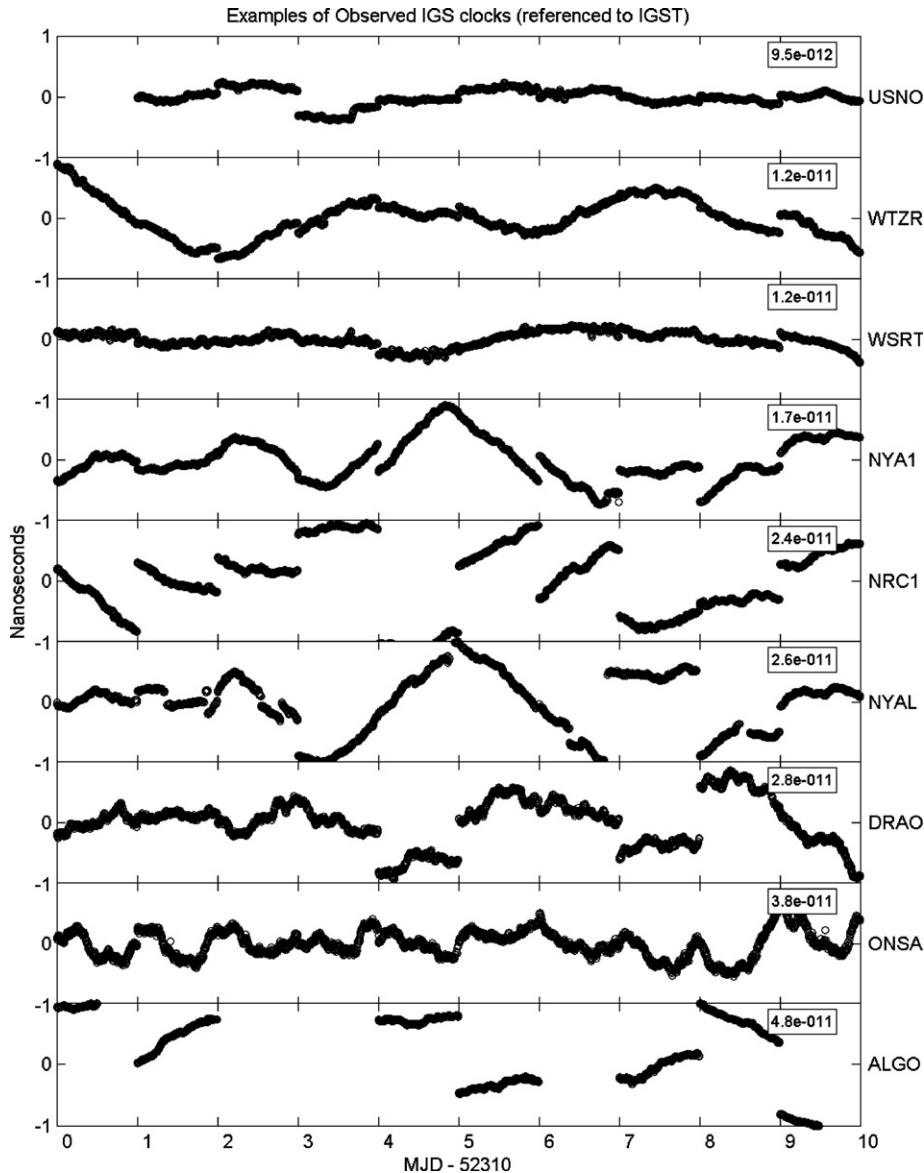


**Figure 5.** Clock estimates of nine IGS sites with H-masers during 5–15 February 2002. A separate quadratic trend has been removed from each clock for plotting. The boxed value in each panel gives the Allan deviation at 300 s, neglecting clock jumps at day boundaries. The magnitude of the day-boundary jumps varies greatly among the stations and is independent of the sub-daily clock stability.

Figure 6 shows the history of the day-boundary clock jumps for those IGS stations at timing labs equipped with H-masers (indicated in table 2 by TL). OPMT has been omitted due to its very sparse data. The BRUS installation, especially since summer 2003, should be considered exemplary and a model for other timing labs.

### 6. Comparisons with independent two-way time transfer results

In addition to the internal assessments discussed above, it is important to compare geodetic clock estimates with those from independent systems. Conventional CV, while widely deployed at timing labs, is not sufficiently accurate to provide very informative comparisons except possibly over the longest averaging intervals. More promising are the P3 CV and two-way satellite time transfer (TWSTT) methods. Some of

the best results over inter-continental baselines demonstrate agreements with geodetic clocks to about 0.5 ns RMS or about 0.3 ns TDEV for averaging times up to a few months [51, 52]. Table 3 summarizes results from recent high-quality comparison studies.

TWSTT measurements are relatively sparse compared with continuous GPS data, about four times daily in recent years. Differences are computed by interpolation of the geodetic and P3 CV results to the TWSTT epochs. The P3 CV data reductions have used IGS precise orbits as well as applying model displacements for solid Earth tide motions. A Vondrák smoothing has also been applied to the P3 results, equivalent to a low-pass filter with a cut-off period of about 0.4 days. As noted by Petit and Jiang [52], the differences between simultaneous time series should be a constant for each clock-pair (equivalent to a calibration bias). Therefore, the standard deviation should be a measure of the relative

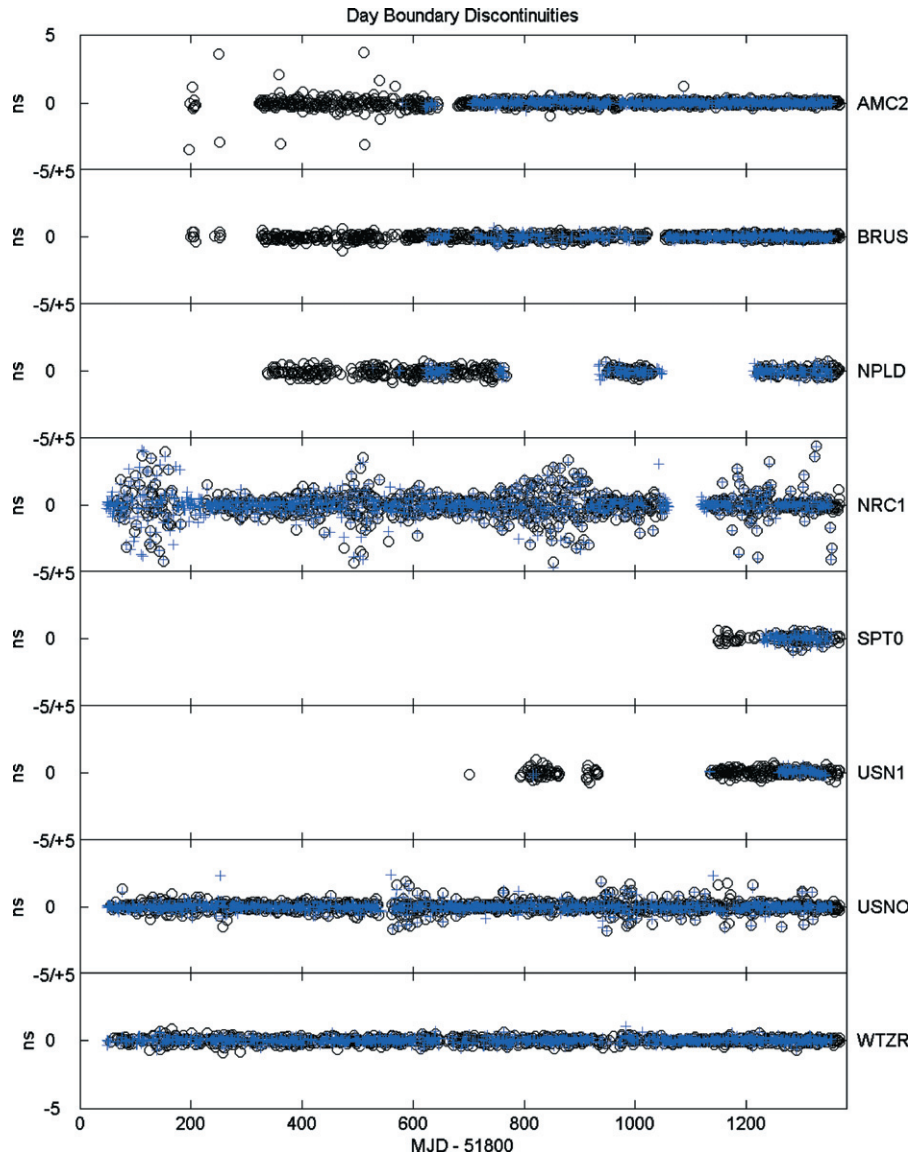


**Figure 6.** Temporal variations in day-boundary clock offsets for eight IGS H-maser stations at timing labs. The study period is October 2000 to June 2004. Results from the IGS Rapid clocks are shown as black circles; Final clocks are blue '+' symbols.

long-term instability of the two time transfer methods. The geodetic and P3 data are often from the same GPS receiver, and so it is expected that some receiver- and antenna-based errors will be common to each and not evident in their differences (such as temperature sensitivity effects). So, only the comparisons with TWSTT are fully independent. For all three of the long baselines studied by Plumb and Larson [51], the Allan deviations of the TW-geodetic clock differences were dominated by TWSTT instabilities up to intervals of  $10^5$  s to  $10^6$  s. At longer intervals, the instabilities of both methods appear very similar.

Based on the published comparisons with TWSTT, the accuracy of geodetic time transfer results is apparently at least as good as  $(0.5 \text{ ns}/\sqrt{2}) = 0.35 \text{ ns}$  (RMS), assuming that each method contributes equally to the observed differences. This is a good deal larger than the geodetic formal errors for 1 day analyses of about  $0.12 \text{ ns}$ , but it is within the range of performance for some poorer GPS stations (see table 2).

Considering that the comparisons also show consistently better stability for geodetic clocks for up to several-day intervals, the actual RMS noise of TWSTT is almost certainly larger and the typical geodetic accuracy is better than  $0.35 \text{ ns}$ .

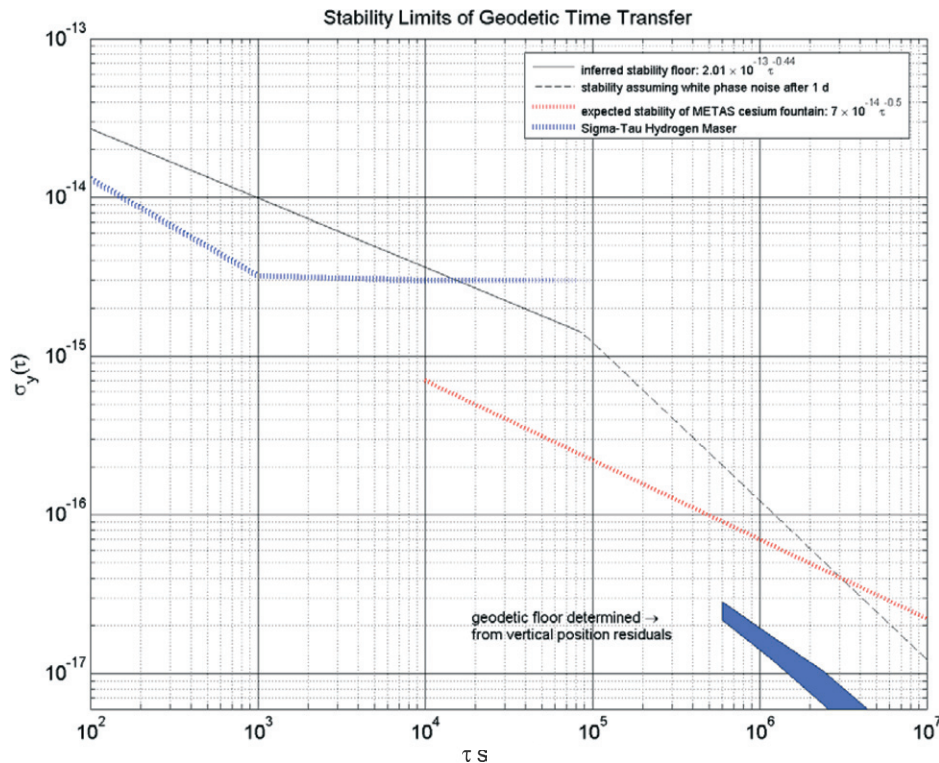
## 7. Assessment of time transfer performance

Figure 7 shows the stability floor of 24 h geodetic clock determinations, as inferred by Ray and Senior [5] from an analysis of IGS clock day-boundary jumps. The behaviour is not significantly different from  $\tau^{-0.5}$ , consistent with a random walk noise process. At an averaging time of 1 day, the inferred instability is  $1.4 \times 10^{-15}$ . Some of the best IGS stations approach this level of performance, but as we have seen, others are much poorer. Beyond the 1 day analysis interval, the clock estimates should be nearly independent and the behaviour is predicted to be closer to that of a white noise process,  $\tau^{-1}$ , as illustrated in figure 7. However, it has not yet been possible

**Table 3.** Summary of published comparisons between geodetic and P3 CV or two-way (TW) satellite time transfer methods for a number of links of varying lengths.

Link	Baseline length	Method/statistic/value	Data span	Source
NPL-PTB	749 km	P3/RMS/0.48 ns TW/RMS/0.57 ns	5 months 4 months	Petit and Jiang [52]
IEN-PTB	835 km	P3/RMS/0.49 ns TW/RMS/0.64 ns	2 months 2 months	Petit and Jiang [52]
TL-CRL	2112 km	P3/RMS/0.58 ns TW/RMS/1.27 ns	8 months 8 months	Petit and Jiang [52]
USNO-NPL	5695 km	P3/RMS/0.48 ns TW/RMS/0.59 ns	5 months 3 months	Petit and Jiang [52]
USNO-PTB	6275 km	P3/RMS/0.45 ns TW/RMS/0.49 ns	5 months 5 months	Petit and Jiang [52]
USNO-AMC <sup>a</sup>	2361 km	TW/Difference $\pm$ RMS/ -2.10 ns $\pm$ 0.69 ns (cal. agreement) TW/TDEV/ <0.1 ns, 300 s $\leq$ $\tau$ $\leq$ 2000 s <0.34 ns, 2000 s $\leq$ $\tau$ $\leq$ 7 $\times$ 10 <sup>6</sup> s TDEV/0.34 ns at 7 $\times$ 10 <sup>6</sup> s	7 months	Plumb and Larson [51]
USNO-NIST	2405 km	TW/RMS/0.83 ns TW/TDEV/ <0.3 ns, 3600 s $\leq$ $\tau$ $\leq$ 6 $\times$ 10 <sup>6</sup> s <0.72 ns, 6 $\times$ 10 <sup>6</sup> s $\leq$ $\tau$ $\leq$ 7.4 $\times$ 10 <sup>6</sup> s TDEV/0.72 ns at 7.4 $\times$ 10 <sup>6</sup> s	5.5 months	Plumb and Larson [51]
PTB-NIST	7532 km	TW/RMS/0.79 ns TW/TDEV/ <0.5 ns, 2 $\times$ 10 <sup>5</sup> s $\leq$ $\tau$ $\leq$ 7.5 $\times$ 10 <sup>6</sup> s TDEV/0.24 ns at 7.5 $\times$ 10 <sup>6</sup> s	7 months	Plumb and Larson [51]
USNO-PTB	6275 km	RMS/2 ns	2 years	Dach <i>et al</i> [56]

<sup>a</sup> TW and geodetic links calibrated separately for instrumental delays.



**Figure 7.** The Allan deviation stability floor for geodetic time transfers, inferred by Ray and Senior [5], is shown by the solid black line. The behaviour is consistent with a random walk noise process up to 1 day intervals. Beyond that, it is expected that independent daily clock estimates will have white noise-distributed errors and follow a  $\tau^{-1}$  Allan deviation, shown by the dashed black line. For comparison, the red trend indicates the design goal for the METAS Cs fountain [53] and the blue trend is for a Sigma Tau H-maser (from Symmetricon). The fundamental geodetic limit is represented by the lower blue band, based on the repeatability of station height measurements.

to study this domain very carefully due to instabilities in the frequency standards in common use. When a caesium fountain data become more available, the stability of geodetic clocks over intervals longer than 1 day will be exposed; figure 7 plots the design goal for the METAS Cs fountain [53], for instance. If analysis arcs are extended beyond 24 h, then the stability floor will probably be lower than the level shown here, though this has not been demonstrated. On the other hand, doing so will definitely extend the random walk behaviour of geodetic clocks over the same longer intervals and could therefore compromise achieving higher stability over longer times using independent 1 day arcs.

Also shown in figure 7 is the specified stability (presumably conservative) of the MHM2010 active H-maser from Symmetricon (successor to the former Sigma Tau H-maser). This shows that the geodetic method need not be a limitation to comparing such high-performance clocks over 1 day intervals, though time transfer noise does probably dominate over clock instabilities for intervals less than about 14 000 s. The dispersion in 1 day stabilities seen among the IGS H-maser stations—from the level of our inferred stability floor up to about  $10^{-14}$ —is probably a combination of the inherent stability of the local frequency standard (some are old devices and some are not maintained under strict environmental control) and the local pseudorange multi-path conditions.

## 8. Future trends

The application of geodetic methods to global time and frequency transfers is only in its infancy. It is not yet widely used within the timekeeping community. We expect much greater adoption of the technique for international time and frequency comparisons in the future, especially in view of its high performance and modest cost. Installation of new, more stable laboratory frequency standards will doubtless spur such a trend. Probably the biggest obstacle to wider usage has been the more complex data analysis required by the geodetic approach. While a number of software packages exist and are very commonly used within the positioning communities, they are less well known among timing groups, which is understandable. Almost certainly, the development of simple generic tools for PPP clock solutions will greatly facilitate broader use of geodetic clock estimates.

As the performance limit for geodetic timing is set by the quality of the pseudorange data, especially multi-path effects, any major improvements in the technique will probably be related to reductions in pseudorange and multi-path errors. Refinements in GPS receiver tracking technology and in geodetic antenna design may offer some benefits. Better siting and installation of existing equipment, including improved temperature stabilization, would certainly be useful in many cases. But the largest gains will likely come with new GNSS broadcast signals and modulation schemes. Some of the proposed signal designs for GALILEO, for instance, offer the prospect of greatly reduced multi-path error [54]. Generally, proposed signal structures which shift more of the power towards the band edges, including some new GPS modulations, promise the potential of significantly improved multi-path mitigation [55].

For time comparisons using any existing method, hardware calibration uncertainty is the dominant absolute error. The calibration errors are at least an order of magnitude larger than the typical errors of the geodetic clock estimates. The prospects for substantial calibration improvements in the future are unclear.

## Acknowledgments

J Ray thanks the Bureau International des Poids et Mesures for their gracious hospitality during the year he spent as a visiting scientist there. G Petit, J Kouba, R Dach, K Larson and P Defraigne have kindly provided helpful critiques and suggestions, which we greatly appreciate.

## References

- [1] Allan D and Weiss M 1980 Accurate time and frequency transfer during common-view of a GPS satellite *Proc. 1980 IEEE Frequency Control Symp. (Philadelphia)* pp 334–56
- [2] Lewandowski W, Azoubib J, De Jong G, Nawrocki J and Danaher J 1997 A new approach to international time and frequency comparisons: 'All-in-view' multi-channel GPS + GLONASS observations *Proc. Institute of Navigation GPS97 (Kansas City, MO)* pp 1085–91
- [3] Zumberge J F, Hefflin M B, Jefferson D C, Watkins M M and Webb F H 1997 Precise point positioning for the efficient and robust analysis of GPS data from large networks *J. Geophys. Res.* **102** 5005–17
- [4] Schildknecht Th, Beutler G, Gurtner W and Rothacher M 1990 Towards subnanosecond GPS time transfer using geodetic processing techniques *Proc. 4th European Frequency and Time Forum (Neuchatel)* pp 335–46
- [5] Ray J and Senior K 2003 IGS/BIPM pilot project: GPS carrier phase for time/frequency transfer and time scale formation *Metrologia* **40** S270–88
- [6] Petit G, Jiang Z, White J, Beard R and Powers E 2001 Absolute calibration of an Ashtech Z12-T GPS receiver *GPS Solutions* **4** 41–6
- [7] Langley R B 1996 GPS receivers and the observables *GPS for Geodesy* ed P J G Teunissen and A Kleusberg (Berlin: Springer) pp 141–73
- [8] Mader G and Czopek F 2002 Calibrating antenna phase centers *GPS World* **13** 40–6
- [9] Ray J R, Dragert H and Kouba J 2000 Recommendations for handling non-Rogue data *IGS 1999 Technical Reports* Jet Propulsion Laboratory Publication, Pasadena, California, pp 445–1
- [10] Schmid R and Rothacher M 2003 Estimation of elevation-dependent satellite antenna phase center variations of GPS satellites *J. Geodesy* **77** 440–6, doi:10.1007/s00190-003-0339-0
- [11] Schupler B R and Clark T A 2001 Characterizing the behavior of geodetic GPS antennas *GPS World* **12** 48–55
- [12] Byun S H, Hajj G A and Young L E 2002 GPS signal multipath: a software simulator *GPS World* **13** 40–9
- [13] Elósegui P, Davis J L, Jaldehag R T K, Johansson J M, Niell A E and Shapiro I I 1995 Geodesy using the global positioning system: the effects of signal scattering on estimates of site positions *J. Geophys. Res.* **100** 9921–34
- [14] Ray J R and Senior K 2001 Temperature sensitivity of timing measurements using Dorne Margolin antennas *GPS Solutions* **5** 24–30
- [15] Rieck C, Jarlemark P, Jaldehag K and Johansson J 2003 Thermal influence on the receiver chain of GPS carrier phase equipment for time and frequency transfer *Proc. 2003 IEEE Int. Frequency Control Symp. and PDA Exhibition*

- Jointly with the 17th European Frequency and Time Forum (Tampa, Florida, 5–8 May 2003) pp 326–31
- [16] Schupler B R, Allshouse R L and Clark T A 1994 Signal characteristics of GPS user antennas *J. Inst. Navigation* **41** 277–95
- [17] Mader G L 1999 GPS antenna calibration at the National Geodetic Survey *GPS Solutions* **3** 50–8
- [18] Overney F, Schildknecht Th, Beutler G, Probst L and Feller U 1997 GPS Time transfer using geodetic receivers: middle-term stability and temperature dependence of the signal delays *Proc. 11th European Frequency and Time Forum* (Neuchatel, Switzerland: Swiss Foundation for Research in Microtechnology) pp 504–8
- [19] Petit G, Thomas C, Jiang Z, Uhrich P and Taris F 1998 Use of GPS Ashtech Z12T receivers for accurate time and frequency comparisons *Proc. 1998 IEEE International Frequency Control Symp.* (Pasadena, CA: Institute of Electrical and Electronics Engineers) pp 306–14
- [20] Bruyninx C, Defraigne P and Sleewaegen J-M 1999 Time and frequency transfer using GPS codes and carrier phases: onsite experiments *GPS Solutions* **3** 1–10
- [21] Schildknecht Th and Dudle G 2000 Time and frequency transfer: high precision using GPS phase measurements *GPS World* **11** 48–52
- [22] Defraigne P, Petit G and Bruyninx C 2001 Use of geodetic receivers for TAI *Proc. 33rd Precise Time and Time Interval Meeting* (Washington, DC: The US Naval Observatory) pp 341–8
- [23] Estey L H and Meertens C M 1999 TEQC: the multi-purpose toolkit for GPS/GLONASS data *GPS Solutions* **3** 42–9
- [24] Choi K, Bilich A, Larson K M and Axelrad P 2004 Modified sidereal filtering: implications for high-rate GPS positioning *Geophys. Res. Lett.* **31** L22608  
doi: 10.1029/2004GL021621
- [25] Petit G, Jiang Z, Moussay P, White J, Powers E, Dudle G and Uhrich P 2001 Progresses in the calibration of ‘geodetic like’ GPS receivers for accurate time comparisons *Proc. 15th European Frequency and Time Forum* (Neuchatel, Switzerland) pp 164–6
- [26] White J, Beard R, Landis G, Petit G and Powers E 2001 Dual frequency absolute calibration of a geodetic GPS receiver for time transfer *Proc. 15th European Frequency and Time Forum* (Neuchatel, Switzerland) pp 167–72
- [27] Plumb J, Larson K, White J and Powers E 2005 Validation of a carrier phase GPS time-transfer system: calibration *IEEE Trans. Ultrason. Ferroelectr. Freq. Control* **52** at press
- [28] Petit G, Jiang Z, Uhrich P and Taris F 2000 Differential calibration of Ashtech Z12-T receivers for accurate time comparisons *Proc. 14th European Frequency and Time Forum* (Turin) pp 40–4
- [29] Counselman C C III and Shapiro I I 1979 Miniature interferometric terminals for Earth surveying *Bull. Geod.* **53** 139–63
- [30] Bossler J D, Goad C C and Bender P L 1980 Using the global positioning system (GPS) for geodetic positioning *Bull. Geod.* **54** 553–63
- [31] Lichten S and Border J 1987 Strategies for high precision GPS orbit determination *J. Geophys. Res.* **92** 12751–62
- [32] Kedar S, Hajj G A, Wilson B D and Heflin M B 2003 The effect of the second order GPS ionospheric correction on receiver positions *Geophys. Res. Lett.* **30** 1829,  
doi: 10.1029/2003GL017639
- [33] Fliegel H, Gallini T and Swift E 1992 Global positioning system radiation force model for geodetic applications *J. Geophys. Res.* **97** 559–68
- [34] Beutler G, Brockmann E, Gurtner W, Hugentobler U, Mervart L and Rothacher M 1994 Extended orbit modeling techniques at the CODE processing center of the International GPS Service for Geodynamics (IGS): theory and initial results *Manuscripta Geodaetica* **19** 367–86
- [35] McCarthy D D and Petit G 2004 IERS Conventions 2003 *IERS Technical Note 32* (Frankfurt am Main: Verlag des Bundesamts für Kartographie und Geodäsie) p 127
- [36] Altamimi Z, Sillard P and Boucher C 2002 ITRF2000: a new release of the International Terrestrial Reference Frame for Earth science application *J. Geophys. Res.* **107** 2214,  
doi: 10.1029/2001-JB000561
- [37] Wu J T, Wu S C, Hajj G A, Bertiger W I and Lichten S M 1993 Effects of antenna orientation on GPS carrier phase *Manuscripta Geodaetica* **18** 91–8
- [38] Kouba J 2004 Improved relativistic transformations in GPS *GPS Solutions* **8** 170–80, doi: 10.1007/s10291-004-0102-x
- [39] Kouba J and Heroux P 2000 Precise point positioning using IGS orbit products *GPS Solutions* **5** 12–28
- [40] Kouba J 2003 A guide to using International GPS Service (IGS) products, <ftp://igsceb.jpl.nasa.gov/igsceb/resource/pubs/GuidetoUsingIGSProducts.pdf>
- [41] Dach R, Beutler G, Hugentobler U, Schaer S, Schildknecht T, Springer T, Dudle G and Probst L 2003 Time transfer using GPS carrier phase: error propagation and results *J. Geodesy* **77** 1–14, doi: 10.1007/s00190-002-0296-z
- [42] Senior K, Matsakis D and Powers E 1999 Attenuating day-boundary discontinuities in GPS carrier-phase time transfer *Proc. 31st Precise Time and Time Interval Meeting* pp 481–9
- [43] Petit G, Jiang Z, Taris T, Uhrich P, Barillet R and Hamouda F 1999 Processing strategies for accurate frequency comparison using GPS carrier phase *Proc. 1999 Joint European Frequency and Time Forum and 1999 IEEE Int. Frequency Control Symp.* pp 235–8
- [44] Bruyninx C and Defraigne P 1999 Frequency transfer using GPS codes and phases: short- and long-term stability *Proc. 31st Precise Time and Time Interval Meeting* (Washington, DC: The US Naval Observatory) pp 471–80
- [45] Larson K M, Levine J, Nelson L M and Parker T E 2000 Assessment of GPS carrier-phase stability for time-transfer applications *IEEE Trans. Ultrason. Ferroelectr. Freq. Control* **47** 484–94
- [46] Dach R, Schildknecht T, Hugentobler U, Bernier L-G and Dudle G 2005 Continuous geodetic time transfer analysis methods *IEEE Trans. Ultrason. Ferroelectr. Freq. Control* submitted
- [47] Kouba J and Springer T 2001 New IGS station and satellite clock combination *GPS Solutions* **4** 31–6
- [48] Senior K, Koppang P and Ray J 2003 Developing an IGS time scale *IEEE Trans. Ultrason. Ferroelectr. Freq. Control* **50** 585–93
- [49] Thomas C and Azoubib J 1996 TAI computation: study of an alternative choice for implementing an upper limit of clock weights *Metrologia* **33** 227–40
- [50] Senior K, Ray J and Petit G 2004 Comparison of instrumental and empirical station timing biases for a set of Ashtech GPS receivers *Proc. 2004 European Frequency and Time Forum* (Guildford) at press
- [51] Plumb J and Larson K 2005 Validation of a carrier phase GPS time-transfer system: estimation strategies and long-term comparisons with TWSTT *IEEE Trans. Ultrason. Ferroelectr. Freq. Control* **52** at press
- [52] Petit G and Jiang Z 2004 Study of time transfer methods: II. TWSTT vs geodetic clock comparisons *Internal BIPM Reports* 28 May 2004 and 16 July 2004
- [53] Dudle G, Joyet A, Berthoud P, Mileti G and Thomann P 2001 First results with a cold cesium continuous fountain resonator *IEEE Trans. Instrum. Meas.* **50** 510–14
- [54] Hein G W and Pany T 2002 Architecture and signal design of the European satellite navigation system Galileo—Status December 2002 *J. Global Position. Syst.* **1** 73–84
- [55] Weill L R 2003 How good can it get with new signals? Multipath mitigation *GPS World* **14** 106–13
- [56] Dach R, Schildknecht T, Springer T, Dudle G and Probst L 2002 Continuous time transfer using GPS carrier phase *IEEE Trans. Ultrason. Ferroelectr. Freq. Control* **49** 1480–90